This paper describes objective technical results and analysis. Any subjective views or opinions that might be expressed in the paper do not necessarily represent the views of the U.S. Department of Energy or the United States Government.

Examples of Uncertainties of Molecular Dynamics Simulations

SAND2018-5262C

World Congress on Computational Mechanics
Symposium: Modeling and Design with Materials Variabilities due to Nano / Microstructure
July 22 – 27, 2018, New York City

X. W. Zhou, R. B. Sills, M. E. Foster, R. A. Karnesky, and R. E. Jones
Sandia National Laboratories, USA

Sandia National Laboratories is a multi-mission laboratory managed and operated by National Technology and Engineering Solutions of Sandia, LLC., a wholly owned subsidiary of Honeywell International, Inc., for the U.S. Department of Energy's National Nuclear Security Administration under contract DE-NA-0003525. The views expressed in the article do not necessarily represent the views of the U.S. Department of Energy or the United States Government.

Outline

1. Statistical uncertainty of molecular dynamics/statics (MD/MS) models
2. Methods of MD/MS uncertainty quantifications
3. Examples
   - ➢Finite-temperature lattice constant calculations
   - ➢Finite-temperature cubic elastic constant calculations
   - ➢Alloy stacking-fault energy calculations
   - ➢Dislocation core energy calculations
   - ➢Diffusivities calculations

X. Zhou, and S. M. Foiles, in "Uncertainty Quantification and Model Calibration", Ed. J. P. Hessling, p. 89 (INTECH, Rijeka, Croatia, 2017).

Observation of MD/MS Uncertainties

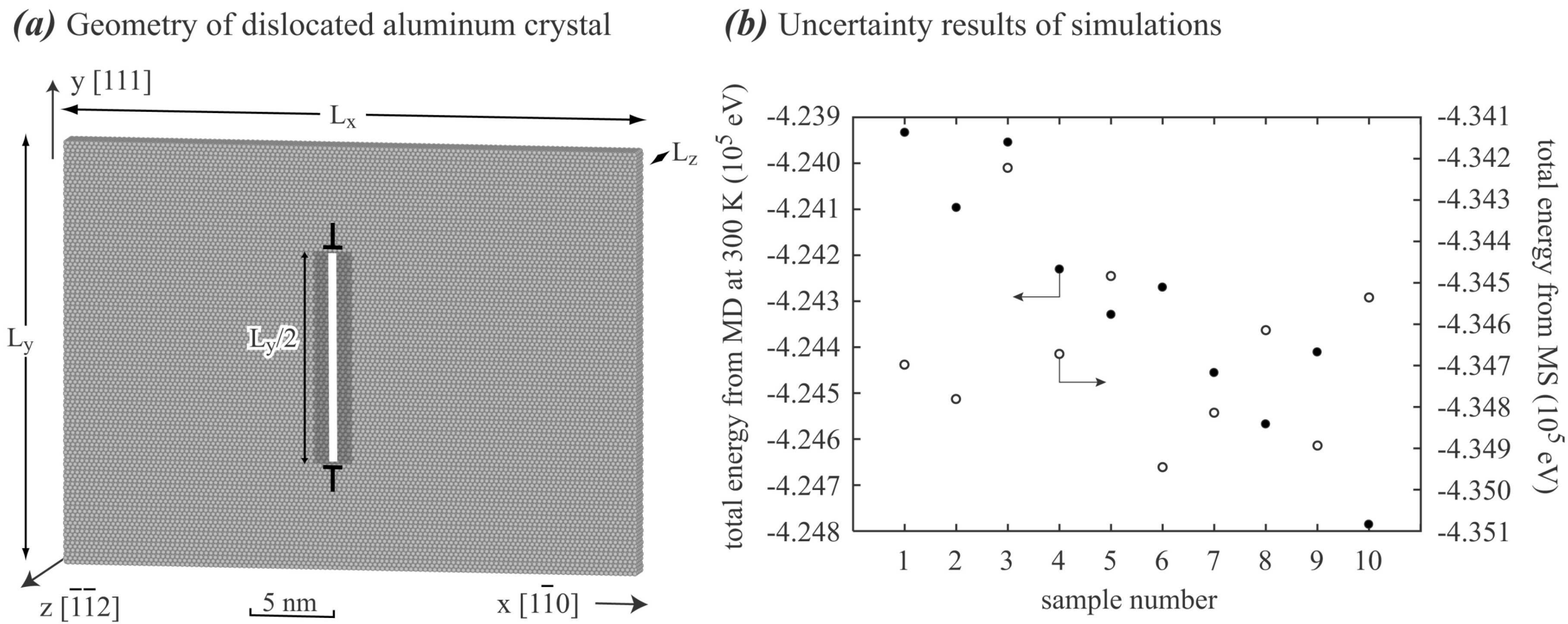

Uncertainties arise from (a) total properties (e.g., energy), (b) large systems (129600 atoms in this case), and (c) distributed low energy configurations of defects

MD Uncertainty Quantification

1. If the same property P_i is time-averaged within different MD simulated time segments $t_i = i\Delta t$ (i = 1, 2, …, N), then the best estimate of the property is $\bar{P} = \frac{\sum_{i=1}^{N} P_i}{N}$. The uncertainty of $\bar{P}$ can be defined by the standard deviation $\sigma = \sqrt{\frac{\sum_{i=1}^{N}(P_i - \bar{P})^2}{(N-1)N}}$
2. If time-averaged $\bar{P}_i$ are obtained for different properties i = 1, 2, …, n, then the uncertainty can also be quantified by $\sigma = \sqrt{\frac{\sum_{i=1}^{n}(\bar{P}_i - P^*)^2}{n}}$, where P^* is knowledge-based relation for these properties. For example:

$$\sigma = \sqrt{\frac{\sum_{i=1}^{3}\left(\bar{a}_i - \sqrt[3]{\bar{a}_1\bar{a}_2\bar{a}_3}\right)^2}{3}}, \sigma = \sqrt{\frac{\sum_{i=1}^{3}\left(\bar{C}_{ii} - \frac{\bar{C}_{11}+\bar{C}_{22}+\bar{C}_{33}}{3}\right)^2}{3}}, \sigma = \sqrt{\frac{\sum_{i=1}^{n}\left[ln\bar{D}_i - \left(lnD_0 - \frac{Q}{kT_i}\right)\right]^2}{n}}$$

for cubic lattice constant, cubic elastic constants, and diffusivities at different temperatures respectively

Finite-Temperature Lattice Constant

$$\xi = \sigma = \sqrt{\frac{\sum_{i=1}^{3}\left(\bar{a}_i - \sqrt[3]{\bar{a}_1\bar{a}_2\bar{a}_3}\right)^2}{3}}$$

(a) Convergence of lattice constant and cohesive energy

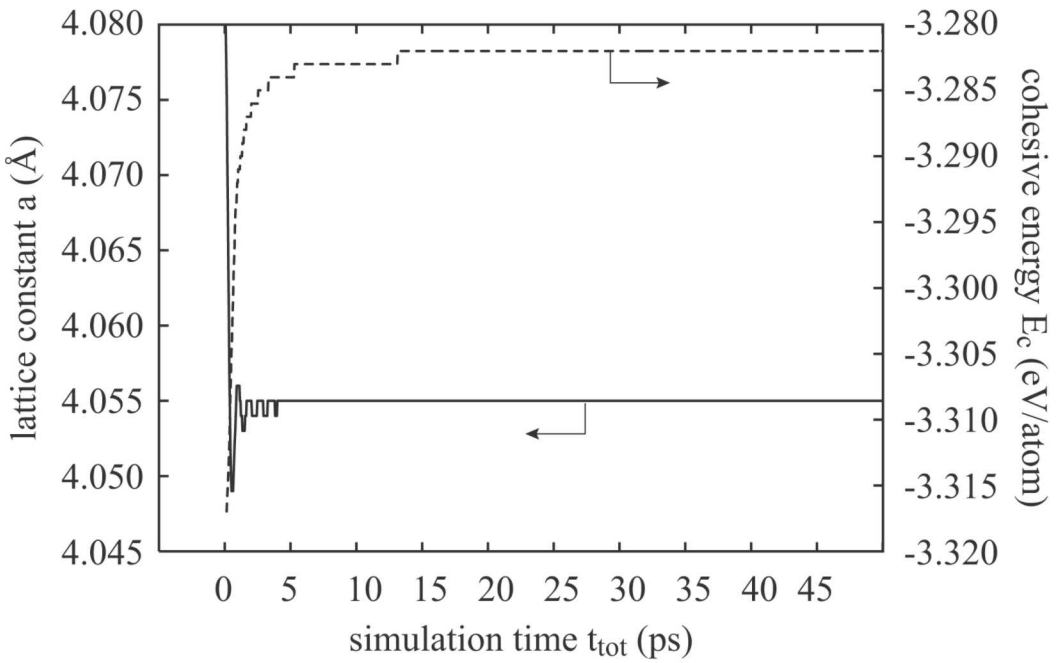

(b) ξ error of lattice constant

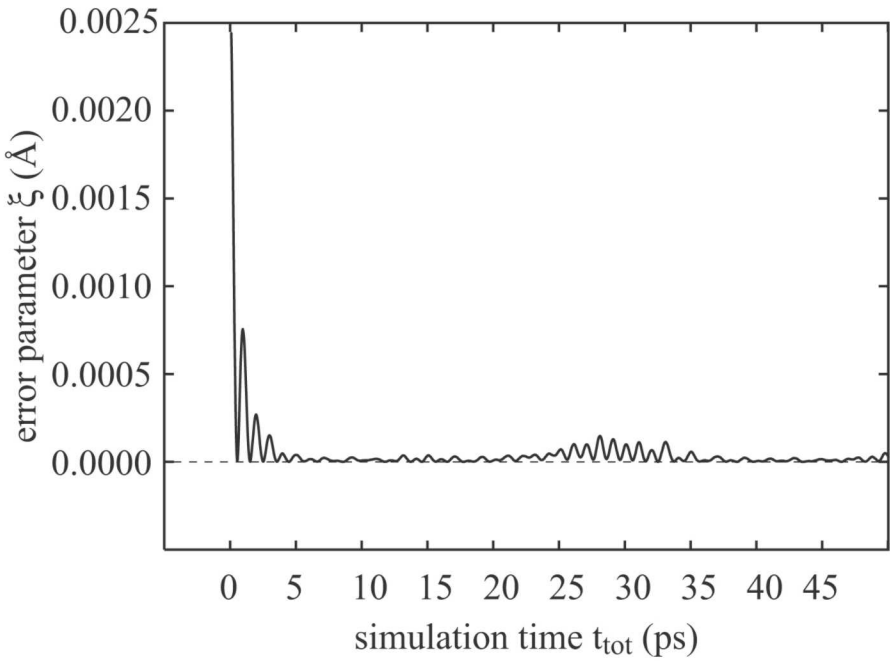

Finite-Temperature Cubic Elastic Constants

$$\xi_1 = \sqrt{\frac{\sum_{i=1}^{3}[C_{ii} - (C_{11} + C_{22} + C_{33})/3]^2}{3}} \qquad \xi_2 = \sqrt{\frac{\sum_{j=1}^{3}\sum_{\substack{i=1 \\ i\neq j}}^{3}\left[C_{ij} - (C_{12} + C_{13} + C_{21} + C_{23} + C_{31} + C_{32})/6\right]^2}{6}}$$

$$\xi_3 = \sqrt{\frac{\sum_{i=4}^{6}[C_{ii} - (C_{44} + C_{55} + C_{66})/3]^2}{3}} \qquad \xi_4 = \sqrt{\frac{\sum_{j=4}^{6}\sum_{i=1}^{j-1}(C_{ij} + C_{ji})^2}{24}}$$

(a) Convergence of elastic constants

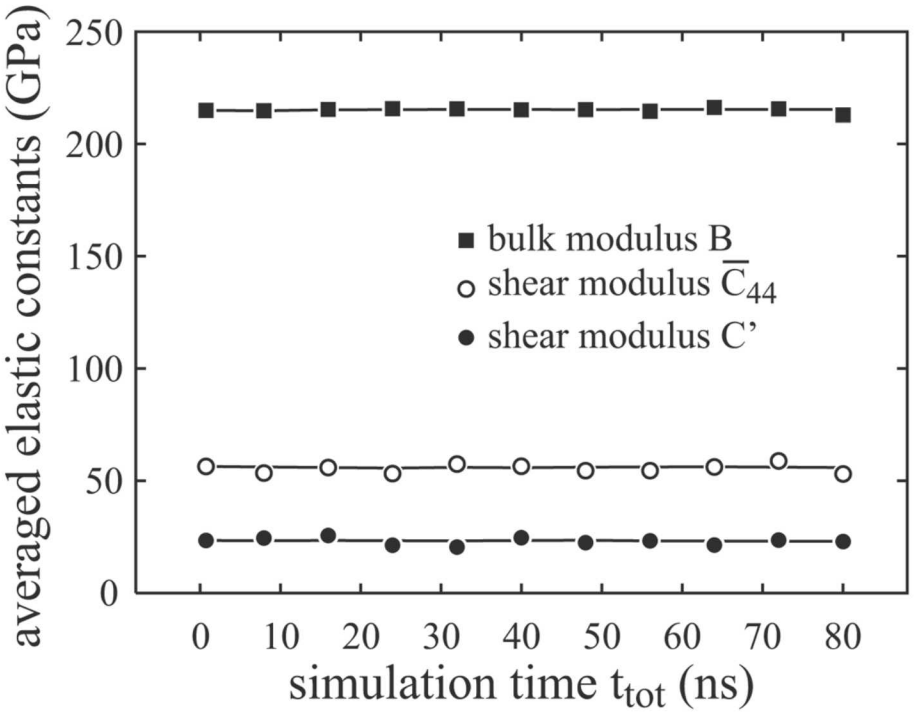

(b) Convergence of physical errors

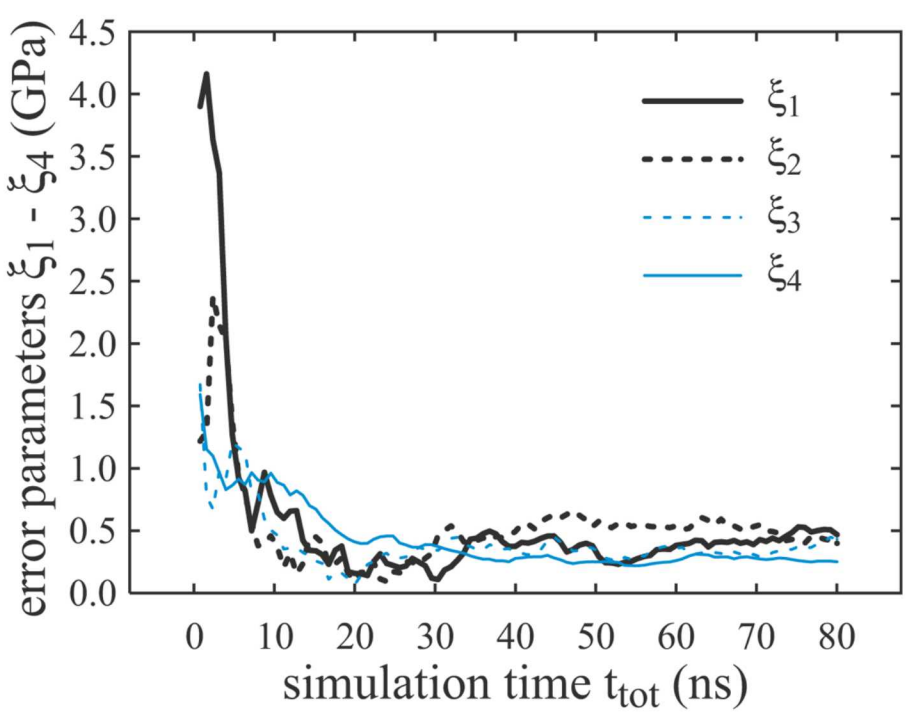

Finite-Temperature Alloy Stacking Fault Energy

(a) Convergence of MD stacking fault energy

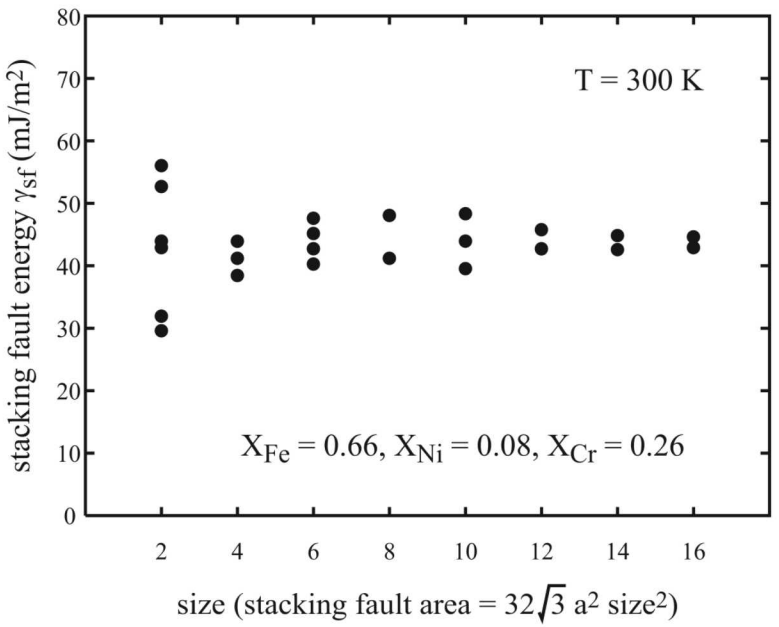

(b) Converged MD stacking fault energy vs. X_{Ni}

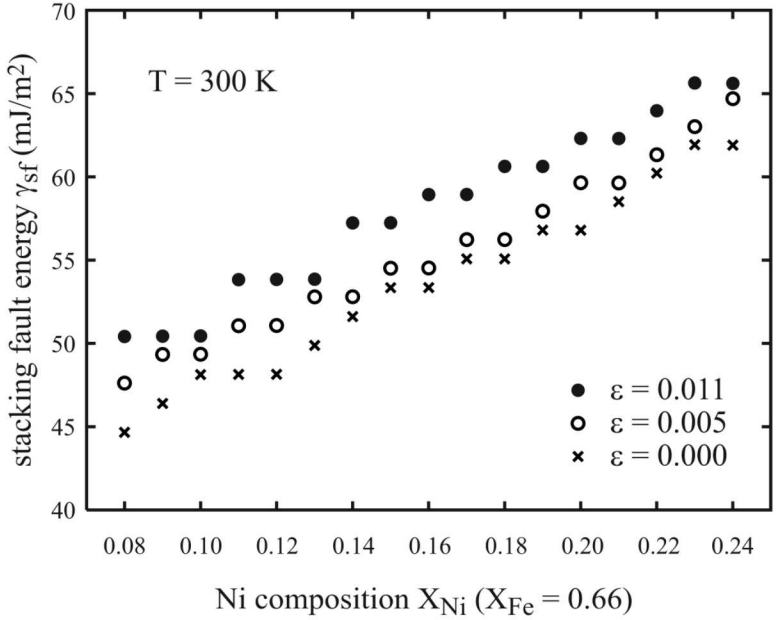

(c) DFT (EMTO-CPA) stacking fault energy vs. X_{Ni}

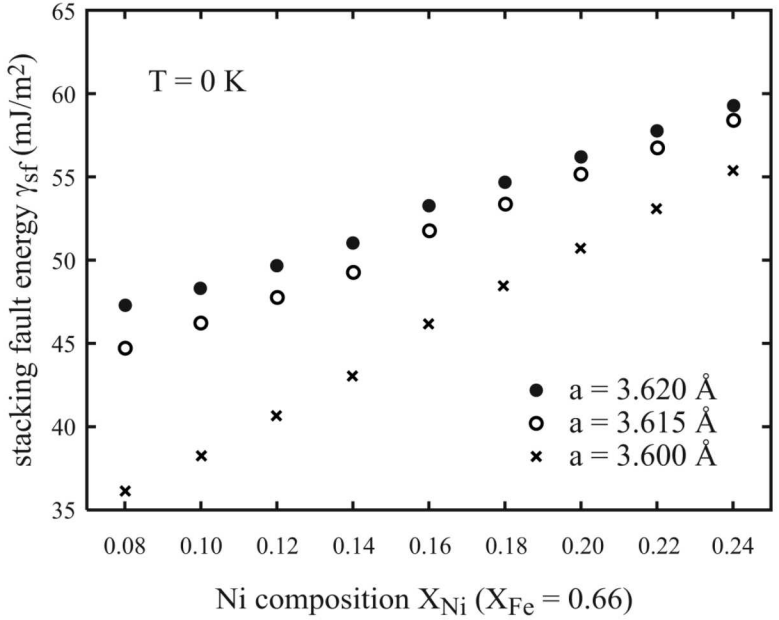

Fe-Ni-Cr EAM, temperature: 300 K, system size: 1179648 atoms, t_{MD}: 0.4 ns

The predicted stacking fault energies match well with experimental results (see, for example, Vitos et al, PRL 2006, 96, 117210, and references therein).

Dislocation Energy: Accuracy in Concept

1. Dislocation cores must be calculated from atomistics, with boundary conditions addressing long range strain fields
2. One way is to fix the boundary atoms to the continuum solutions
   - Dislocation type unknown
   - Anisotropic calculations required
   - Boundary atoms for dislocated and perfect systems non-identical
3. Another way is to use periodic boundary conditions
   - Dislocation type accurately captured
   - Continuum calculations not required
   - Boundary atoms for dislocated and perfect systems consistent
   - No approximation is introduced regardless dislocation array configuration

Dislocation Energy: History of Periodic Methods

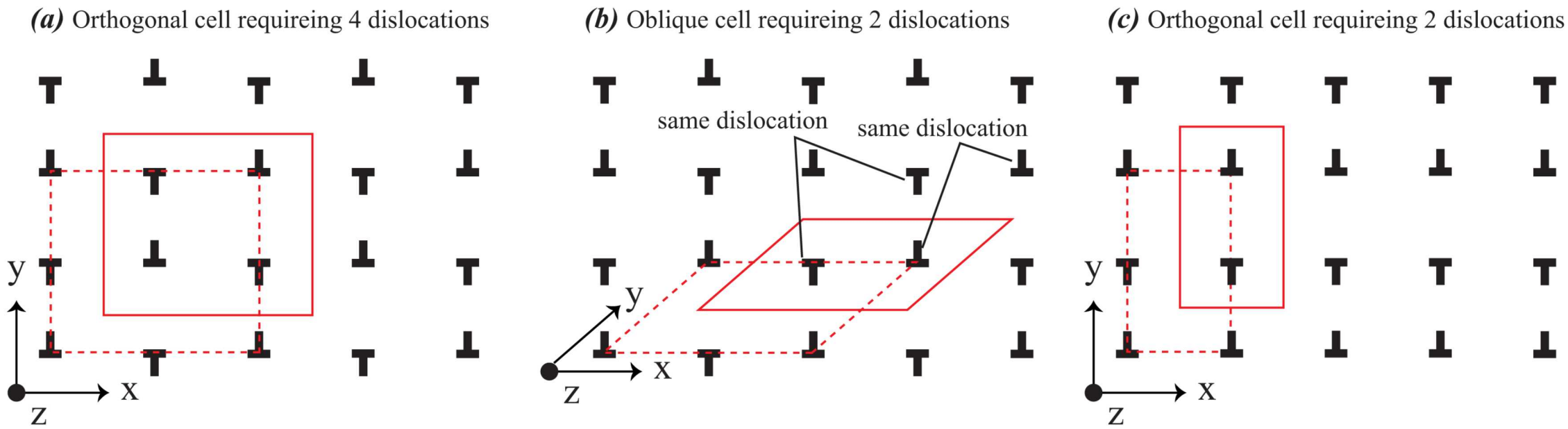

1. Traditionally quadruple dislocations shown in the left image are used (Bigger et al, PRL, 1992, 69, 2224)
   - Dislocations may annihilate
2. Quadruple dislocations can be implemented with oblique cell in the middle image
   - Literature only acknowledges the computational efficiency
   - Annihilation is more difficult
3. Single dipole configurations in the right image eliminate annihilation
   - Used successfully by Cai et al (e.g., PRL, 2001, 86, 5727)
   - Also successfully used by us

Difference between Our and Literature Methods

1. Method of periodic boundary conditions with only one dipole is not clear in Cai et al's papers
2. There is a conditional convergence problem in Cai et al's configuration
   - Experts' experiences are required to deal with this
3. Literature methods are limited by statistical errors
4. Our methods (Zhou et al, PRB, 2017, 95, 054112; JMPS, 2016, 91, 265; Uncertainty Quantification and Model Calibration, INTECH, Rijeka, Croatia, 2017) solved all the three problems above
   - Methods of periodic boundary conditions are simple and are described
   - Analytical expression for dislocation dipole arrays are derived
   - Time-averaged molecular dynamics reduces statistical errors

Dislocation Geometry

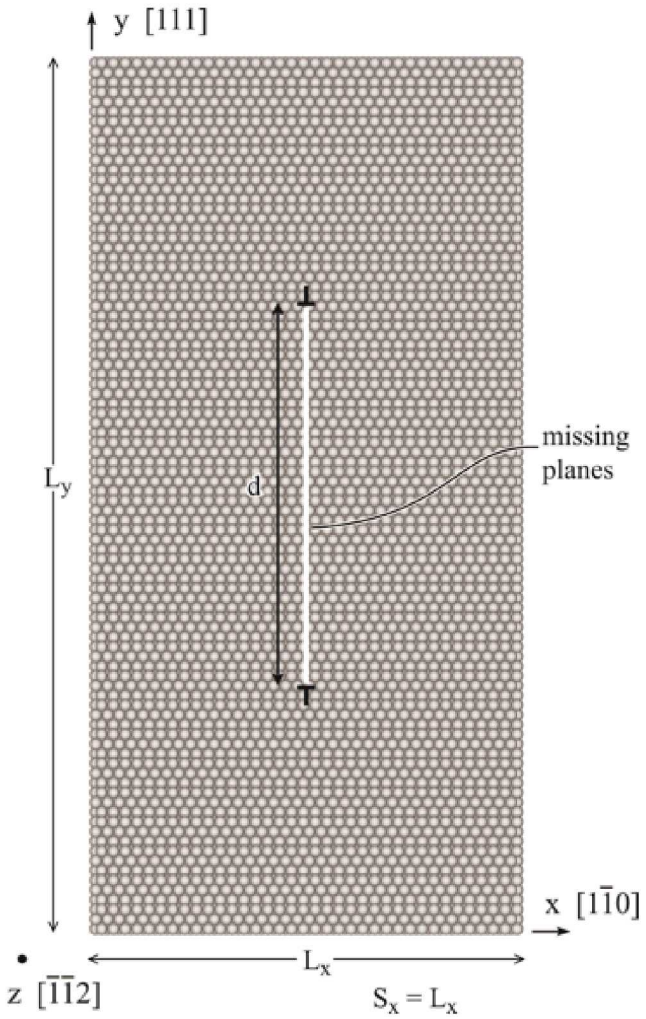

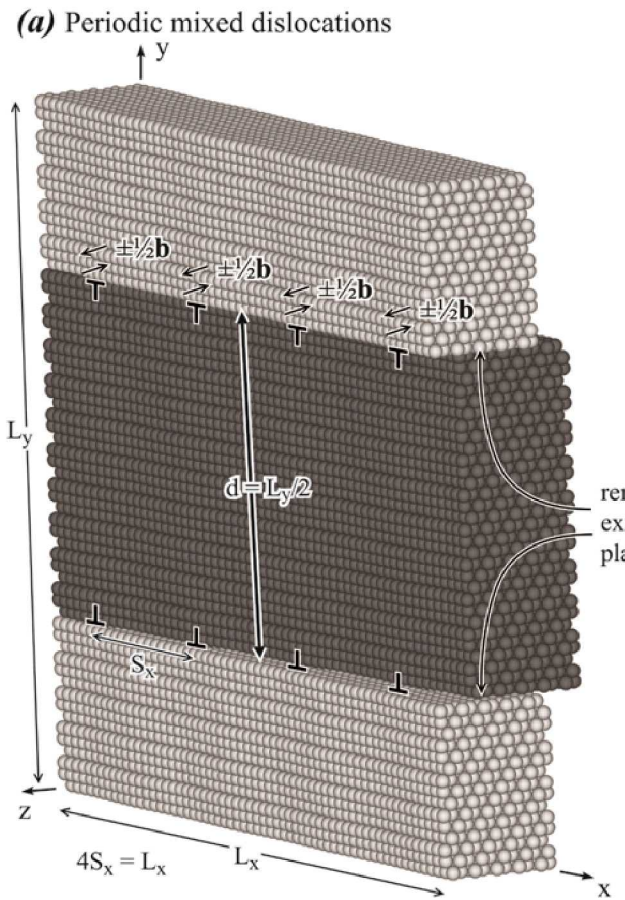

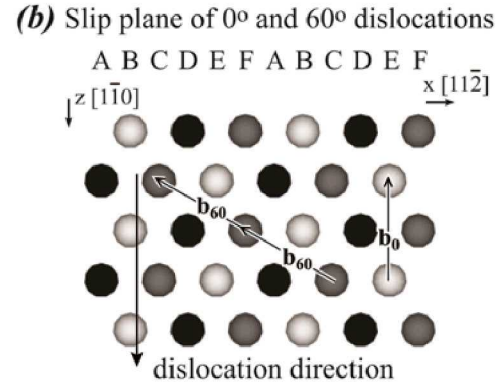

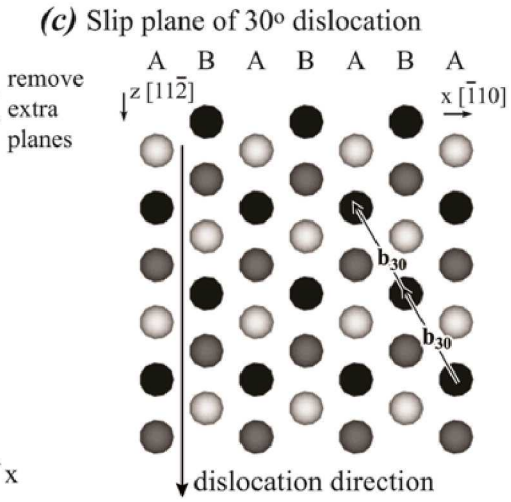

1. One dipole for edge dislocations
2. Multiple dipoles for other dislocations
3. Orthogonal cell can be used
4. Orthogonal cell, however, requires that $d = L_y/2$ for non-edge dislocations

Time-Averaged MD Calculations

CdS Dislocation Energy

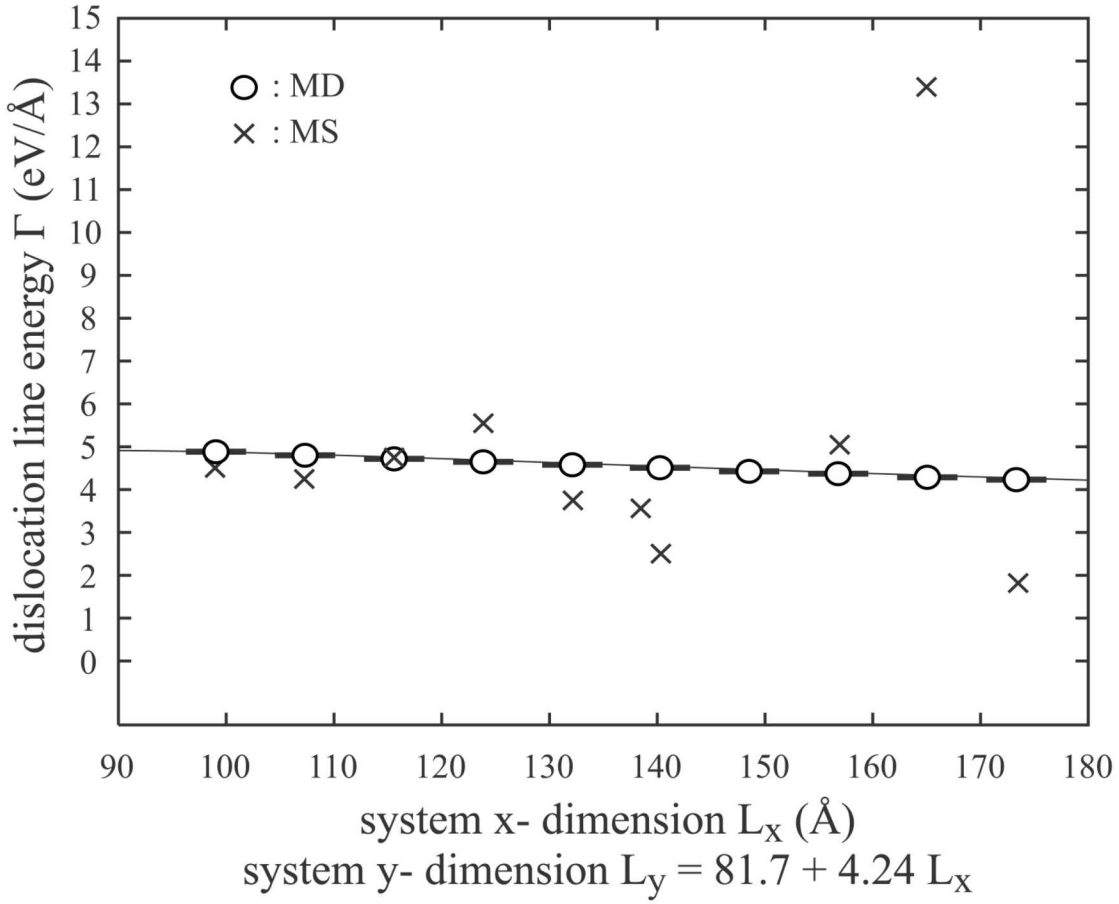

1. All literature calculations use molecular statics simulations at zero K
2. No literature calculations use big cells
3. We found that statistical errors of molecular statics simulations are too large for large systems (X. Zhou, and S. M. Foiles, in "Uncertainty Quantification and Model Calibration", Ed. J. P. Hessling, p. 89 (INTECH, Rijeka, Croatia, 2017)
4. Time-averaged molecular dynamics can reduce statistical errors

temperature: 300 K, the largest system size: 141120 atoms, t_{MD}: 16 ns

Continuum Energy Expression

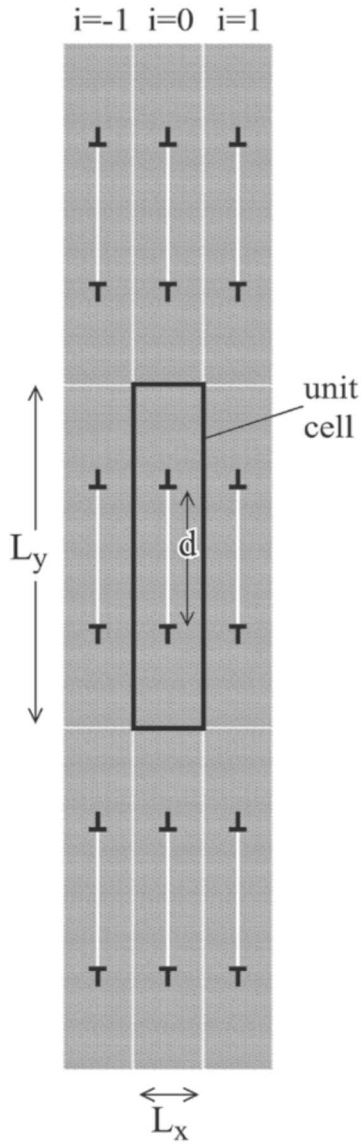

$$\Gamma = E_c + \frac{Gb^2}{4\pi(1-\nu)} \cdot \cos^2\alpha + \sin^2\beta \cdot E_{0,edge} + \cos^2\beta \cdot E_{0,screw} + 2\sin^2\beta \cdot \sum_{i=1}^{\infty} E_{i,edge} + 2\cos^2\beta \cdot \sum_{i=1}^{\infty} E_{i,screw}$$

$$E_{0,edge} = \frac{Gb^2}{4\pi(1-\nu)}\left\{\ln\left(\frac{d}{r_0}\right) + \ln\left(\frac{L_y - d}{L_y}\right) - \ln\left[Ga\left(\frac{L_y + d}{L_y}\right)\right] - \ln\left[Ga\left(2 - \frac{d}{L_y}\right)\right]\right\}$$

$$E_{0,screw} = \frac{Gb^2}{4\pi}\left\{\ln\left(\frac{d}{r_0}\right) + \ln\left(\frac{L_y - d}{L_y}\right) - \ln\left[Ga\left(\frac{L_y + d}{L_y}\right)\right] - \ln\left[Ga\left(2 - \frac{d}{L_y}\right)\right]\right\}$$

$$E_{i,edge} = \frac{Gb^2}{8\pi(1-\nu)}\left\{\begin{array}{l} \dfrac{4\pi \cdot i \cdot L_x \cdot \coth\left(\dfrac{\pi \cdot i \cdot L_x}{L_y}\right) \cdot \sin^2\left(\dfrac{\pi \cdot d}{L_y}\right)}{L_y \cdot \cosh\left(\dfrac{2\pi \cdot i \cdot L_x}{L_y}\right) - L_y \cdot \cos\left(\dfrac{2\pi \cdot d}{L_y}\right)} + \\ \ln\left[\cos^2\left(\dfrac{\pi \cdot d}{L_y}\right) + \coth^2\left(\dfrac{\pi \cdot i \cdot L_x}{L_y}\right) \cdot \sin^2\left(\dfrac{\pi \cdot d}{L_y}\right)\right] \end{array}\right\}$$

$$E_{i,screw} = \frac{Gb^2}{8\pi}\ln\left[\cos^2\left(\frac{\pi \cdot d}{L_y}\right) + \coth^2\left(\frac{\pi \cdot i \cdot L_x}{L_y}\right) \cdot \sin^2\left(\frac{\pi \cdot d}{L_y}\right)\right]$$

E_c independent of geometry!

- E_c, r_0: core energy, radius
- Ga: Euler gamma function
- coth, cosh: hyperbolic functions
- G, ν: shear modulus, Poisson's ratio
- b: Burgers magnitude
- α: dislocation dipole direction (α = 0° means vertical dislocation dipole)
- β: dislocation character angle

Aluminum Edge Dislocation Results

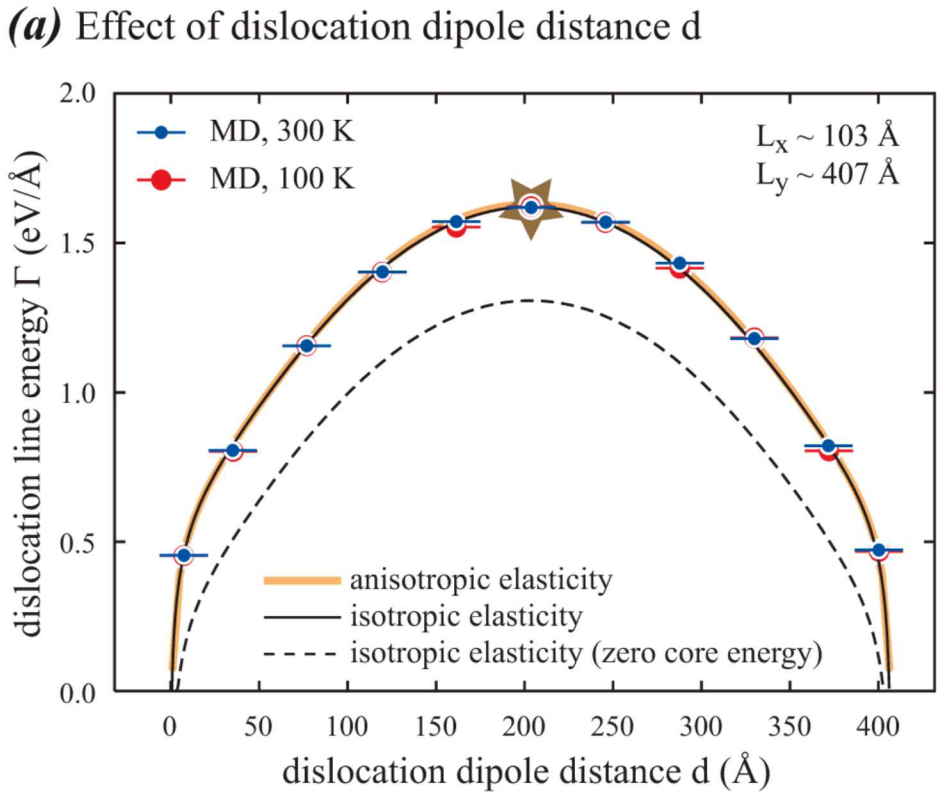

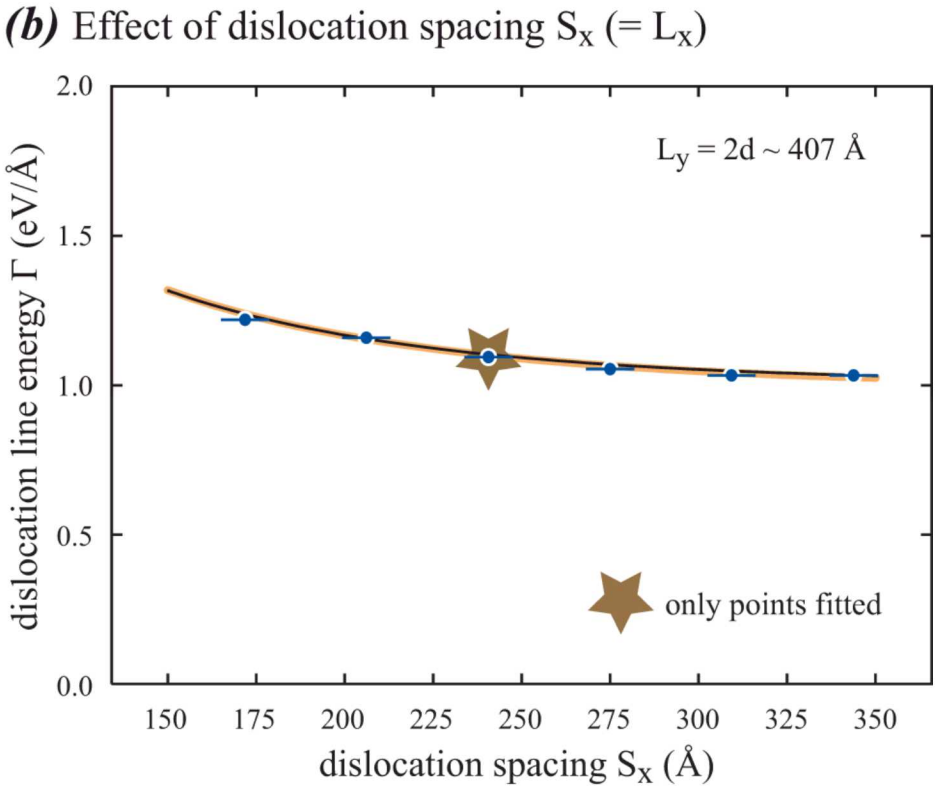

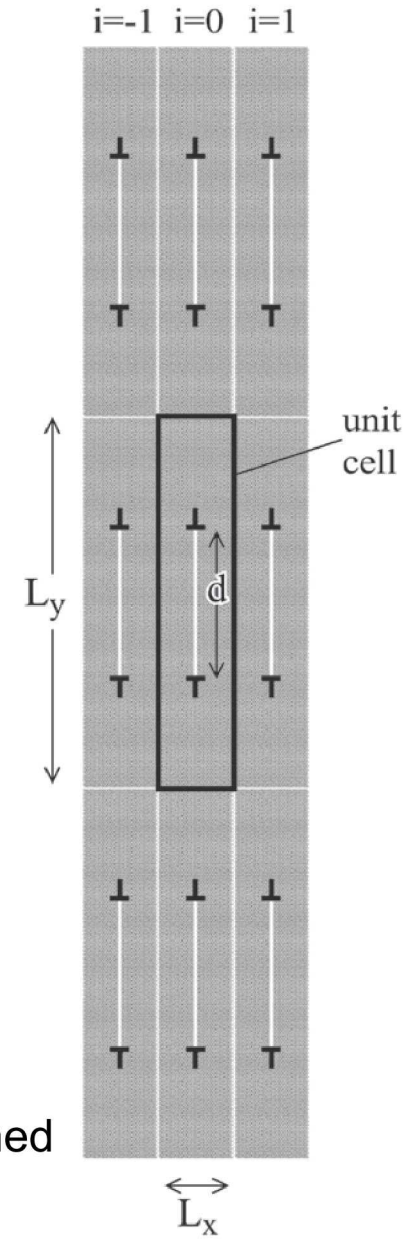

1. Continuum dislocation energy = $\Gamma(G,\nu,b,r_0,E_c,\beta,d,L_x,L_y)$
2. Simulations provide Γ values at a variety of (β,d,L_x,L_y)
3. Dislocation core radius r_0 can be any value as long as the energy within r_0 is captured by the E_c
4. By fitting the MD Γ values to the continuum expression at a chosen r_0, (G,ν,E_c) can all be determined
5. Γ is a symmetric function of d (important to validate)

system size: 62640 atoms, t_{MD}: 3.2 ns

Zhou et al, Phys. Rev. B, 95, 054112 (2017)

Aluminum Mixed and Screw Dislocation Results

(a) 30°, 60° dislocations

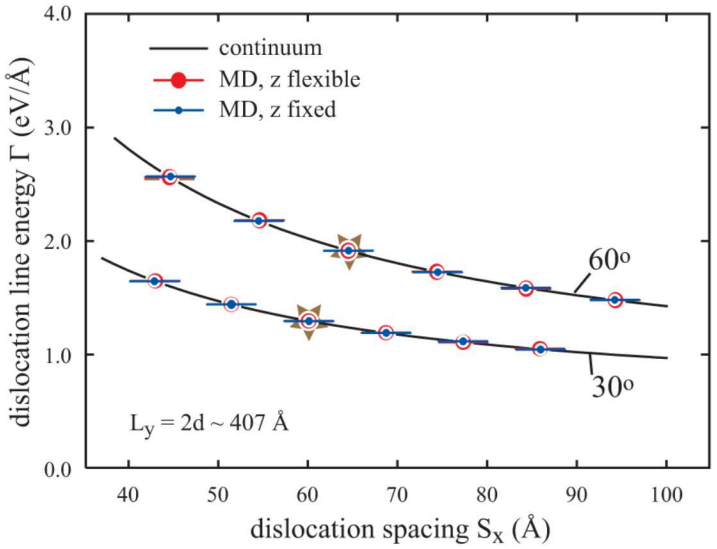

(b) 10.89°, 19.11°, 40.89°, 49.11°, 70.89°, 79.11° dislocations

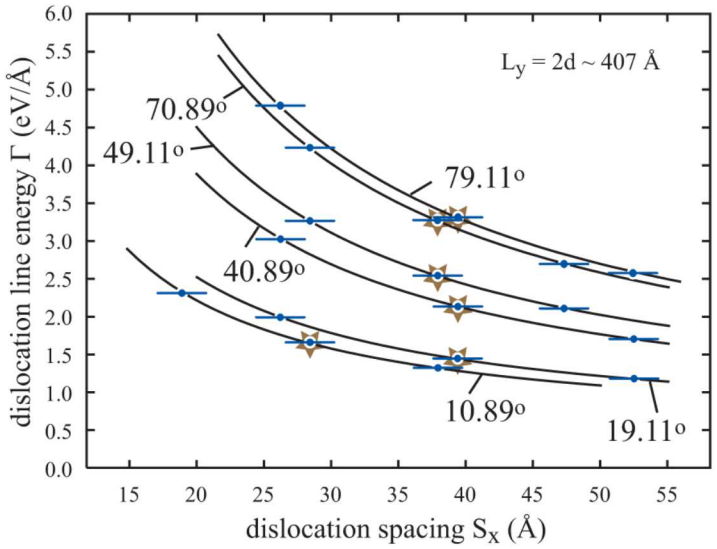

(c) 0.0° (screw) dislocation

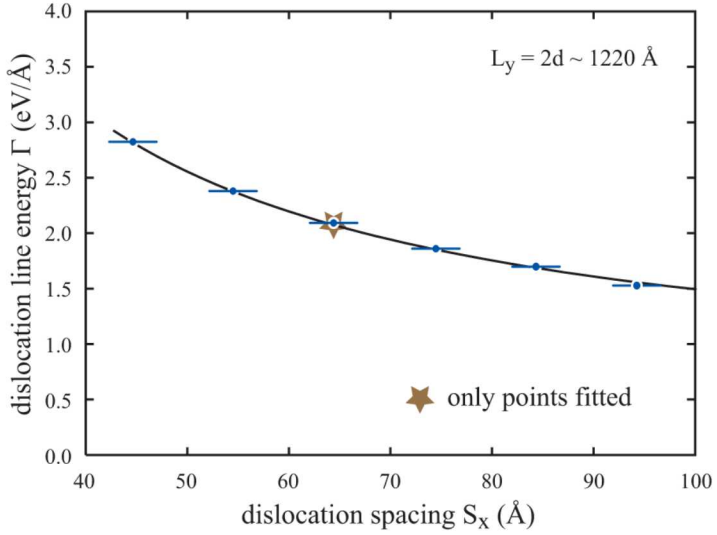

Core energy as a function of character angle

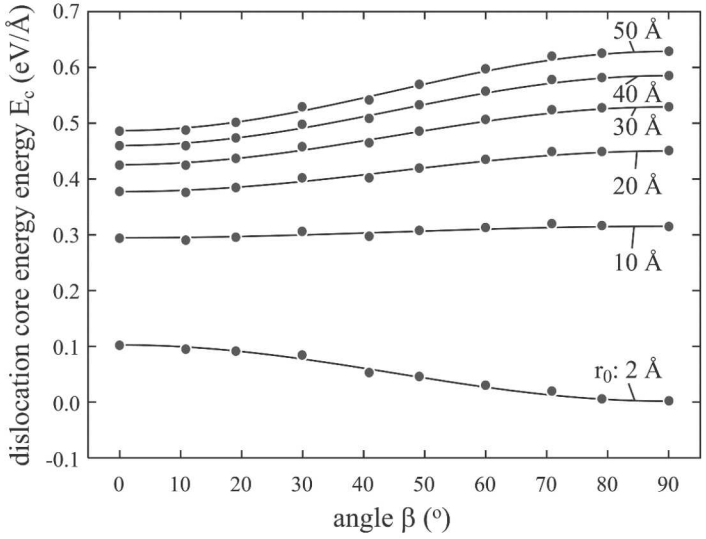

1. There are only N+2 unknowns, (E_c at the N β angles + G + ν), but many more equations
2. All MD data points have zero ~error bars
3. All MD data points fall exactly on continuum lines
4. Converged results lead to derivation of core energy as a function of character angle

the largest system size: 852600 atoms, t_{MD}: > 3.2 ns

Diffusion Analysis Methods

1. The coordinates $\alpha_i(t)$ of N diffusion atoms (i = 1, 2, …, N), are recorded on a time interval of Δt, i.e., at times of $t = j\Delta t$, j = 1, 2, …, m ($m = t_{MD}/\Delta t$), where Δt can be any multiple of the time step size dt used in the MD simulations.
2. m+1-k measurements can be made for the displacement of a diffusion atom i over a $k\Delta t$ period: $\Delta\alpha_{i,j}(k\Delta t) = \alpha_i(j\Delta t-\Delta t+k\Delta t) - \alpha_i(j\Delta t-\Delta t)$ where j = 1, 2, …, m+1-k.
3. This allows us to calculate mean square displacement (MSD):

$$\left\langle \left[\Delta\alpha(k\Delta t)\right]^2 \right\rangle = \frac{\sum_{i=1}^{N}\sum_{j=1}^{m+1-k}\left[\Delta\alpha_{i,j}(k\Delta t)\right]^2}{N(m+1-k)}$$

4. MSD can be fitted to diffusivities D:

$$\left\langle \left[\Delta\alpha(k\Delta t)\right]^2 \right\rangle = 2D_\alpha t$$
$$\left\langle \left[\Delta x(k\Delta t)\right]^2 \right\rangle + \left\langle \left[\Delta z(k\Delta t)\right]^2 \right\rangle = 4D_{xz} t$$
$$\left\langle \left[\Delta x(k\Delta t)\right]^2 \right\rangle + \left\langle \left[\Delta y(k\Delta t)\right]^2 \right\rangle + \left\langle \left[\Delta z(k\Delta t)\right]^2 \right\rangle = 6D_{xyz} t$$

Molecular statics simulation of individual atomic jump path no longer works

MSD

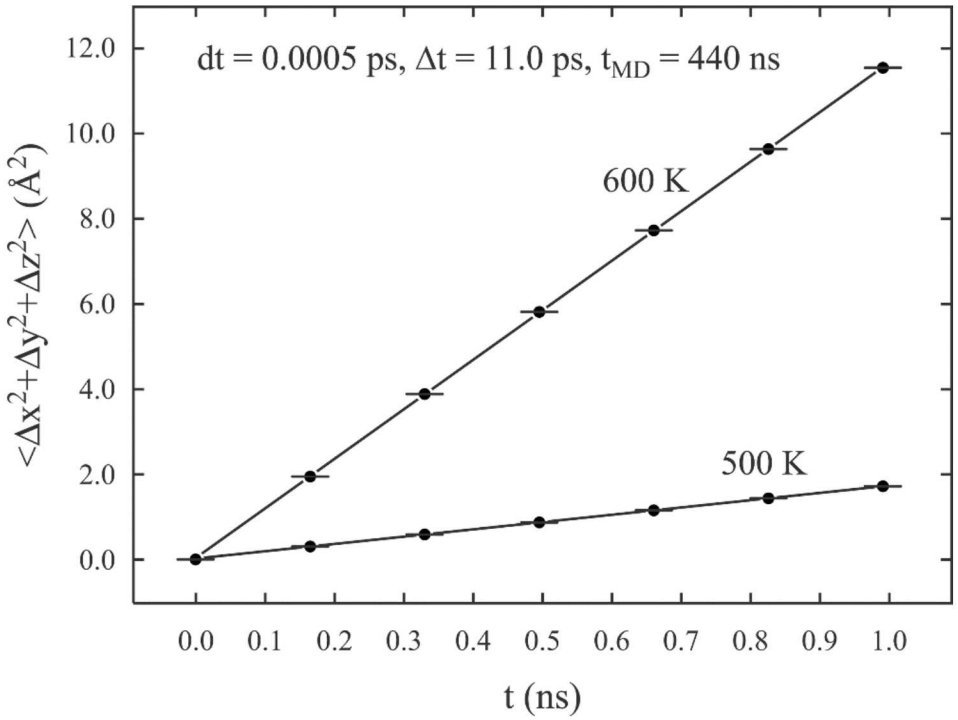

Arrhenius Plots

system size: 2048 Pd atoms, t_{MD} = 2.2 ns

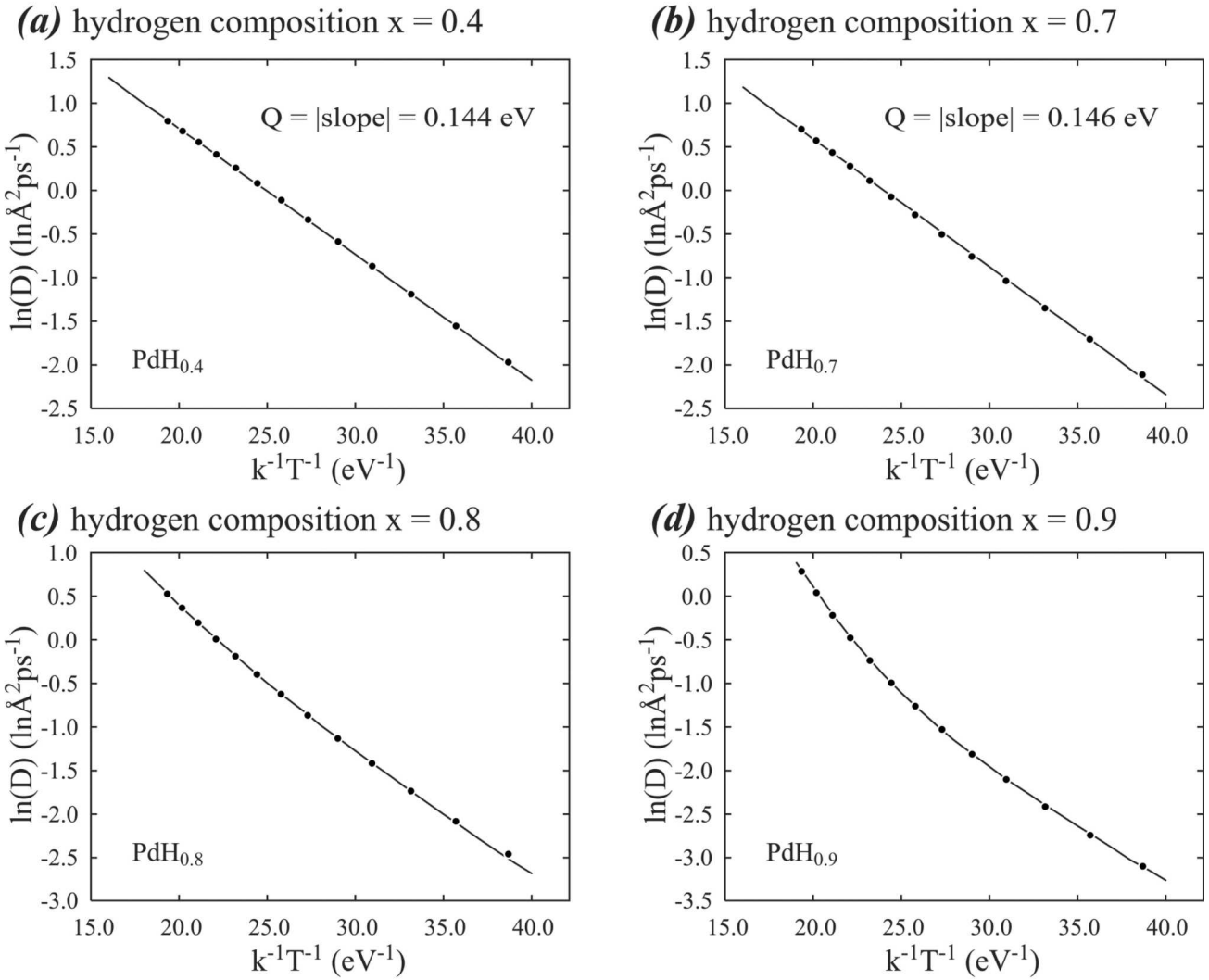

Experiments (Arons et al)

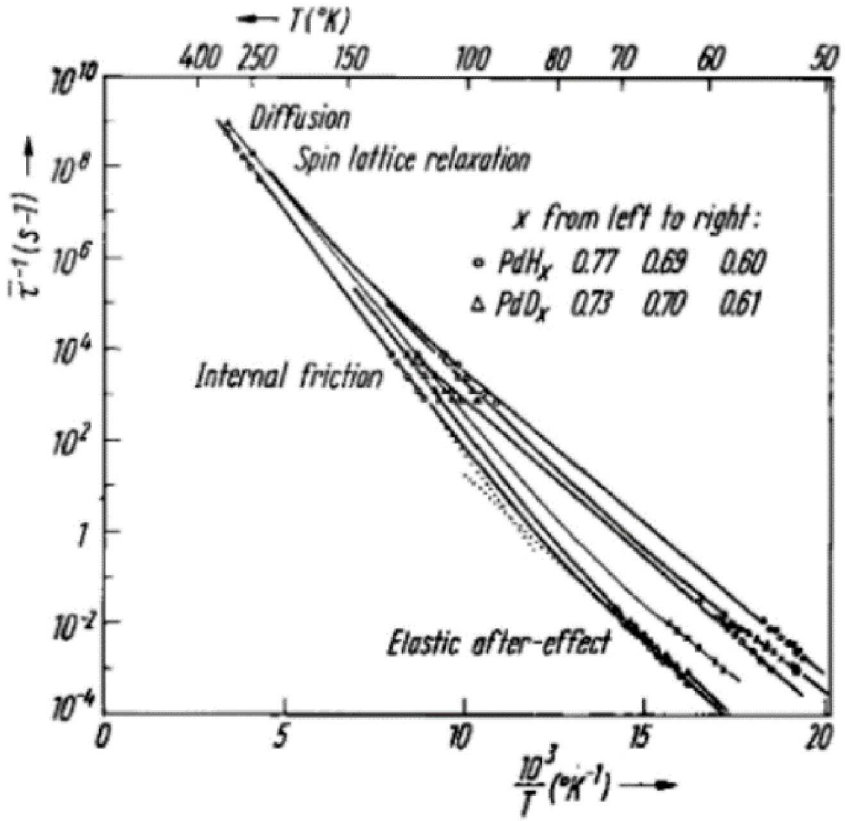

1. MD results exactly on lines
2. Statistical errors negligible
3. No time/length scale issues
4. Linear Arrhenius at low H
5. Non-linear Arrhenius at high H

Zhou et al, Scripta Mater., 149, 103 (2018); Arons et al, Solid State Commun., 14, 1203 (1974); Phys. Status Solidi, 40, 107 (1970).

Conclusions

1. Two methods can be used to quantify uncertainties of MD simulations
2. For large systems, MS simulations may have significant statistical errors
3. Time-averaged MD simulations significantly reduce statistical errors
4. For periodic problems, statistical errors of time-averaged MD simulations can always be reduced to negligible level without time/length scale issues
5. Challenges: non-periodic problems, inaccuracy of interatomic potentials